The Monte Carlo Method: Versatility Unbounded In A Dynamic Computing World
Chattanooga, Tennessee, April 17–21, 2005, on CD-ROM, American Nuclear Society, LaGrange Park, IL (2005)

INVESTIGATION OF QUASIRANDOM SEQUENCES FOR SIMULATING NEUTRAL PARTICLE TRANSPORT

James Tickner*
CSIRO Minerals
PMB 5, Menai, NSW 2234, Australia
James.tickner@csiro.au

ABSTRACT

Quasirandom (QR) sequences are finding increasing application in the evaluation of multidimensional integrals. Compared to integration using pseudorandom sequences with a convergence rate of $N^{-0.5}$ (where N is the number of trials), integration using QR sequences can converge as fast as N^{-1}, although the improvement is highly problem dependent. The application of QR sequences to particle transport has received relatively little attention, with most work focusing on 1-dimensional problems. A computer code has been written simulating two-group neutral particle transport, whose physics includes isotropic elastic and inelastic scattering and absorption. The code allows complex 3-dimensional geometry models to be simulated, includes variance reduction tools and a range of commonly used tally estimators. The code allows otherwise identical simulations to be carried out using pseudo- or quasirandom sequences. Results from running the code on a suite of test problems are presented. For simple cases, a convergence rate close to N^{-1} is observed, decreasing as the problem complexity increases.

Key Words: Neutral particle transport, quasirandom numbers, quasi Monte Carlo, QMC

1 INTRODUCTION

The slow convergence of pseudorandom Monte Carlo methods for simulating particle transport is well known. The Monte Carlo method consists of simulating a series of particle histories from a particle's "birth" from a radiation source to when the particle and any daughter products have been absorbed or discarded. The starting point and subsequent movement through position/momentum phase space is pseudorandomly sampled from the appropriate physical distributions. Suppose that N particle histories are simulated and that the contribution of the i^{th} history to a tally of interest is f_i. Then the best estimate of f averaged over all histories is given by

$$\langle f \rangle = \frac{1}{N} \sum_{i=1}^{N} f_i \tag{1}$$

The expected value of the error on f due to averaging over only N histories is given by

$$Err(f) = \sqrt{\frac{\langle f^2 \rangle - \langle f \rangle^2}{N}} \tag{2}$$

* Tel. +61 2 9710 6732, Fax. +61 2 9710 6789

The angle brackets in equations (1) and (2) denote averaging over the N simulated histories. We recognize the denominator in equation (2) as the variance of the set of f values. The variance can often be reduced by careful selection of the estimator used to evaluate the tally of interest and by appropriate application of non-analogue games (sampling from biased rather than physical distributions, with appropriate weighting of the sampled particles). These so-called variation reduction methods can lead to significant improvements in efficiency. However, the slow, $O(1/\sqrt{N})$ error convergence remains which can make the Monte Carlo method prohibitively expensive.

Quasirandom (QR) sequences have been widely explored as an alternative to pseudorandom numbers for the numerical evaluation of multidimensional integrals. QR sequences are designed to yield numbers that are more uniformly distributed than pseudorandom sequences and can be terminated at any stage whilst preserving this uniform distribution property. Despite their name, QR sequences are strictly deterministic and have long-range correlations, such that later numbers in the sequence "fill in" the gaps left by earlier numbers. James, Hoogland and Kleis [1] have written an excellent review of QR sequences for multidimensional integration and simulation.

Suppose we wish to estimate the integral of a function $f(x_1, x_2, \ldots, x_s)$ over the unit (hyper)cube $x_i \in [0,1] \forall i = 1, s$. If f is evaluated at N randomly selected points, the best estimate of the value of the integral of f is given by equation 1. If the N points at which f is evaluated are chosen pseudorandomly, then the expected error on the integral of f is given by equation 2. However, if the N values of $x_1, x_2 \ldots x_s$ are chosen from s independent QR sequences, the increased uniformity in the distribution of points at which f is evaluated can lead to a more rapid convergence in the expected error. For optimal cases, the error can converge as fast as N^{-1}.

The correspondence between multidimensional integration and particle simulation is straightforward. The tally contribution f_i corresponding to particle history i can be written as the value of the function f evaluated at the point $x_1, x_2, x_3 \ldots$ where the coordinate x_j corresponds to the j^{th} random number used in the generation of the history. The average value of tallied quantity f is equivalent to the integral of f over the unit hypercube and is given by equation 1. Of course, the number of random numbers used will normally vary from history to history, corresponding to a variation in the dimension of f. However, we can consider f to be of fixed dimension s by defining f for history i to be independent of coordinates x_j $(m<j\leq s)$ where m is the number of random numbers used in the i^{th} history. Here s is the maximum number of random numbers used in any of the N simulated histories. Evaluation of a tally by particle transport simulation is thus equivalent to an integral over the unit hypercube and we might hope that the application of QR integration methods might lead to an improvement in the error convergence rate.

The aim of this paper is to explore the application of QR sequences to the simulation of neutral particle transport. Three topics are particularly addressed. Firstly, the choice of the QR sequence generator is discussed. The ideal generator produces uniform deviates with low discrepancy, extends readily to high dimensions, has minimal serial correlations between dimensions, is easy to code and executes rapidly. Secondly, evaluating the integration error is considerably harder than for the pseudorandom case. Existing theoretical error bounds are relatively weak and difficult to estimate. An empirical error estimation method is used, assuming only a power-law convergence rate. Finally, the influence of problem complexity, tally selection and variance reduction on convergence rate is discussed.

2 QR NUMBER GENERATION

Methods for generating QR sequences have been described by many authors, including Halton [2], Sobol [3], Faure [4], Niederreiter [5], and others. There seems to be little consensus as to which, if any, of these sequences offers the best results in the general case; rather the best generator often seems to be problem-dependent. The Halton generator was chosen for the current study due to its straightforward implementation.

The j^{th} element of a standard Halton sequence is constructed by reversing the digits of the integer j expressed in some base b and adding a radix point at before the leftmost digit, yielding a number between 0 and 1. If we deduce the unique set of coefficients $a_i(b,j)$ for which

$$j = \sum_{i=0} a_i(b,j)\, b^i \tag{3}$$

then the j^{th} element of the Halton sequence in base b, $H_b(j)$ is given by

$$H_b(j) = \sum_{i=0} a_i(b,j)\, b^{-(i+1)} \tag{4}$$

For example, the first 7 terms of Halton sequence H_2 are 0.1_2=0.5, 0.01_2=0.25, 0.11_2=0.75, 0.001_2=0.125, 0.101_2=0.625, 0.011_2=0.375 and 0.111_2=0.875. Independent Halton sequences can be constructed using different bases which are mutually prime. Typically, the Halton bases are chosen to be the first s random numbers. If s is small, then the different Halton sequences are found to be largely uncorrelated. Figure 1(a) plots the first 500 points of (H_2,H_3). For comparison, figure 1(b) plots 500 pseudorandom points.

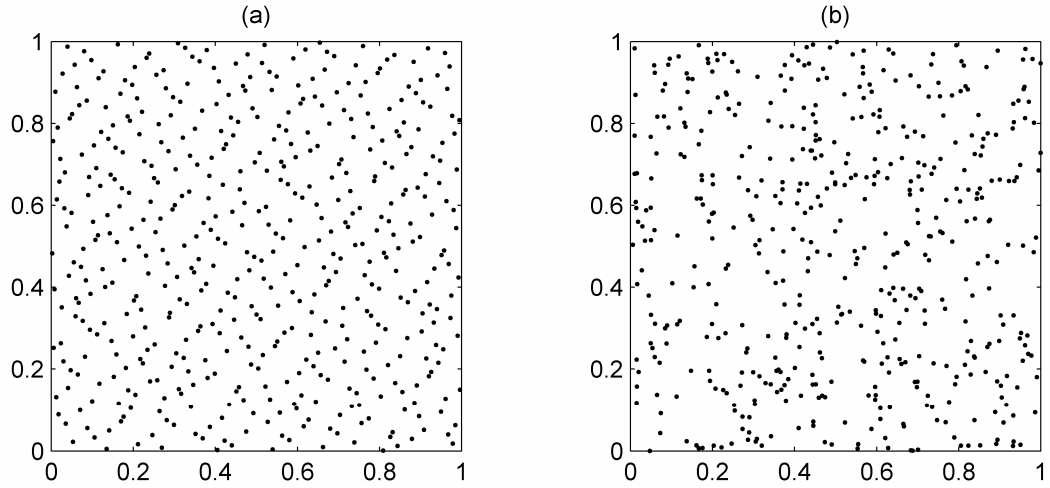

Figure 1. (a) Distribution of 500 points from Halton sequences H_2 and H_3 (b) Distribution of 500 pseudorandom points

It can be seen that the Halton sequence points are more smoothly distributed than the pseudorandom ones. This reflects the low discrepancies of the Halton sequences (see section 3) and accounts for the improved convergence when Halton or other quasirandom sequences are used for numerical integration.

Whilst the lower Halton sequences are quite uncorrelated, the same is not true for higher sequences. For example, figure 2(a) plots the first 500 points of the 19th Halton sequence (b=67) versus the 20th Halton sequence (b=71). A strong correlation between the two sequences is evident and the points fill the unit square very poorly. A significant improvement is achieved by scrambling the coefficients $a_i(b,j)$. Equation (4) is replaced by

$$H_b(j) = \sum_{i=0} \sigma[a_i(b,j)]\, b^{-(i+1)} \tag{5}$$

where σ is the operator of permutations on the $a_i(b,j)$ coefficients which depends on the base b. Kocis and Whiten [6] have proposed a simple scheme for choosing the permutations which is adopted here. Figure 2(b) plots the first 500 points of the digit-scrambled H_{67} and H_{71} sequences. The correlations between the two sequences are significantly reduced.

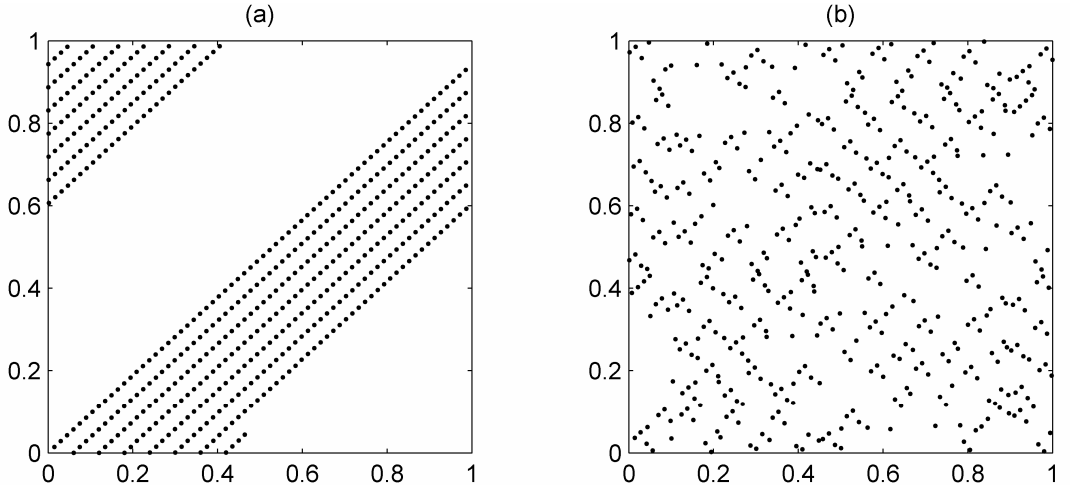

Figure 2. (a) Distribution of 500 points from Halton sequences H_{67} and H_{71}
(b) Distribution of 500 points from digit scrambled Halton sequences H_{67} and H_{71}

An important property of random number generators is that they can be *reseeded* or started from different points in the sequence. The standard Halton sequences always starts at the same point. Wang and Hickernell [7] have demonstrated a simple method for randomising the starting point of a Halton sequence. A number x_0 is chosen pseudorandomly in the range [0,1) and a set of coefficients $a_i(b)$ is found such that

$$x_0 = \sum_{i=0} \sigma[a_i(b)]\, b^{-(i+1)} \tag{6}$$

The expansion is truncated at an appropriate number of digits based on the desired period of the Halton sequence and the floating point precision of the machine used for the sequence computation. The starting point for the Halton sequence H_b, $s_0(b)$ is calculated from equation (3):

$$s_0(b) = \sum_{i=0} a_i(b)\, b^i \tag{7}$$

The j^{th} term of H_b is then given by

$$H_b(j) = \sum_{i=0} \sigma[a_i(b, j + s_0(b) - 1)]\, b^{-(i+1)} \tag{8}$$

In practice, the expansion coefficients $a_i(b,j+1)$ can be calculated directly from the coefficients $a_i(b,j)$. This avoids the need to store and manipulate large integer values and allows the period of the Halton sequences to exceed the maximum machine integer value, typically 2^{32}-1.

3 ERROR ESTIMATION

A significant drawback of QR methods is that no result equivalent to equation (2) is known, which would allow both the best value and error to be calculated from the same point set. The Koksma-Hlawka inequality provides an upper estimate of the maximum integration error, based on the extreme or star-discrepancy D^* of the integration point set and the variation in the sense of Hardy and Krause, V_{HK} of the function being integrated:

$$\left| \int f(\boldsymbol{x})\, d\boldsymbol{x} - \frac{1}{N} \sum_{i=1}^{n} f(\boldsymbol{x}_i) \right| \le V_{HK} \cdot D^*(\boldsymbol{x_1}, \boldsymbol{x_2}, \cdots, \boldsymbol{x_n}) \tag{9}$$

The star-discrepancy is defined by

$$D^*(\boldsymbol{x_1}, \boldsymbol{x_2}, \cdots, \boldsymbol{x_n}) = \sup_A \left| \frac{m(A)}{N} - V(A) \right| \tag{10}$$

where A is a s-dimension hyper-rectangle with edges parallel to the coordinate axes and one vertex at the origin, $V(A)$ is its volume and $m(A)$ is the number of sample points inside this volume. In other words, the star-discrepancy measures the maximum difference between the volume of an arbitrary rectangle A and the fraction of points that it contains. If a point set has a star-discrepancy of D^*, then every rectangle with edges parallel to the coordinate axes and a volume of $2^s D^*$ or larger contains at least one point. For low-discrepancy or QR sequences, D^* can be of order $\log^s(N)/N$, or $\log^{s-1}(N)/N$ if N is fixed before the set is generated.

In practice, the Koksma-Hlawka inequality is of little use for error estimation. Evaluation of the star-discrepancy for anything other than a trivial point set is prohibitively expensive. The variation takes the form of sums of integrals over mixed partial derivatives of the function f and cannot be readily evaluated from a sampled set of points. For functions that are unbounded, or have infinite mixed partial derivatives (that is, discontinuities that are not parallel to the coordinate axes), the variation is infinite. Such functions are common in transport simulation.

Practical methods provide a numerical estimate of the integration error by splitting the integration point set into several subsets and evaluating the integration result for each subset. The final integration result is given by the average of the results for each point subset; the error is given by some measure of the variance of the subset results.

In a total of N integral evaluations are to be used, the simplest method is to split this set into m subsets, each containing N/m points. Each subset comprises points selected from independent QR sequences, for example by pseudorandomly selecting the starting points of the sequences. The subsets are used to make m independent estimates of the desired integral. Denoting these estimates by I_j $(j=1,m)$, the best estimate of the integral $\hat{I} = \int f \, d\boldsymbol{x}$ and the integration error $Err(\hat{I})$ are given by

$$\hat{I} = \frac{1}{m}\sum_{j=1}^{m} I_j \tag{11}$$

$$Err(\hat{I}) = \sqrt{\frac{\sum_{j=1}^{m}(I_j - \hat{I})^2}{m(m-1)}} \tag{12}$$

Unfortunately, this method sacrifices some accuracy. For an integral converging like N^{-1} using a QR point set, the error obtained using m sets each containing N/m points will be $m^{0.5}$ times larger than that obtained using a single set with N points. If m is large enough to make a reasonable estimate of $Err(\hat{I})$, say $m=16$, the integration error will be 4 times larger.

Snyder [8] has described an improved method. A set of N points is chosen using a single QR sequence and is repeatedly partitioned into m = 4, 8, 16, 32 or 64 subsets. The integration error is estimated for each partitioning using equation (12). The error is then extrapolated to $m=1$ using a power-law fit through the errors estimated for $m=4, \ldots, 64$ to provide an estimate for the final integration error. The power-law exponent is restricted to the range 0.5-1.0 which is found to reduce the variance of the error estimate. Care has to be taken to ensure that the partitioned subsets are themselves low discrepancy sequences. For the Halton sequences used in this paper, best results are empirically found to be obtained when each partition consists of a contiguous block of points.

4 DEVELOPMENT OF QR PARTICLE TRANSPORT CODE

A computer code was written simulating 2-group particle transport using either pseudorandom or QR number sequences. The high-quality *ran2* pseudorandom generator described in Numerical Recipes [9] is used. The code is designed so that in addition to reporting the final integration result and error after the total number of events has been simulated, intermediate results are reported to allow the convergence performance to be tested.

4.1 Physics Model

A simple, 2-group, neutral particle physics model is simulated. Particles in either group (A or B) can undergo 3 processes, namely absorption, after which the particle history is terminated, elastic scattering and inelastic scattering where the particle is converted to the other group (B or A).

The elastic and inelastic scattering processes are taken to be isotropic in the laboratory frame. All materials can then be described by 6 parameters, namely the macroscopic cross-sections for absorption, elastic and inelastic scattering for the 2 particle groups. Particles are assumed to be emitted isotropically from a point source. Between interactions, particles travel in straight lines. The distance between interactions is determined by sampling the number of mean free-paths (MFPs) from an exponential distribution and then tracking the particle through the geometry model until the required number of MFPs has been used up. Particles are followed until they are absorbed or they escape from the problem geometry.

Initial generation of the source particle requires two random numbers (the polar and azimuthal angles). Two random numbers are required for each subsequent interaction to sample the number of MFPs to the interaction and the interaction type. If the particle is not absorbed, two further random numbers are required to sample the polar and azimuthal angles of the scattered particle. The dimensionality of the transport simulation is then $4(N_S+1)$ where N_S is the number of times the particle scatters before being absorbed.

4.2 Geometry representation

A full, 3-dimensional, computed solid geometry (CSG) model is used. Simple primitives (rectangular parallelepipeds, cylinders, spheres, prisms and frusta) are specified and volumes in the problem defined in terms of unions, intersections and differences of these primitives. The geometry package provides routines to read in the problem definition from a file, determine the volume that contains a particular point and to calculate the distance to the next volume boundary.

4.3 Tallies and variance reduction

Track length flux, analogue particle current and next-event point flux estimator tallies are permitted. A particle-splitting/Russian roulette game is provided, based on importances assigned to each problem volume. Splitting or killing of particles is performed when they cross the boundary from one volume to the next. Particles are split $\lfloor r \rfloor$ ways if the ratio r of the new to the old volume's importance is greater than 1. Particles are terminated with probability r if r is less than 1. The sampling used to decide whether a particle is killed or not is pseudorandom.

When particle splitting occurs, the split particles are placed on a stack for subsequent tracking. If QR sequences are being used, a note is made of the number of random numbers that have been used so far in the event. When the split particles are tracked, sampling for each one is started at the same point – that is, from the same Halton sequence. This approach reduces the overall dimension of the problem and makes best use of the low-discrepancy nature of each Halton sequence.

5 PERFORMANCE ON PROBLEM TEST SUITE

A suite of problems was developed to test the QR transport code. For each problem, a single run was generated using the pseudorandom *ran2* generator and 50 runs using the QR generator, each reseeded to a different starting point. Each run consisted of 2^{20}=1048576 events. The 50 QR runs allow an independent estimate of the error to be made from the standard deviation of the tally values. Tally and error estimates were reported every 2^n events with $n=12,14, \ldots 20$, making a total of 9 reporting points.

5.1 Problem Suite

The following problems were run:

P1 Mean track length in infinite volume for a 100% absorbing material with unit cross-section

P2 Fraction of particles escaping from unit radius sphere containing a 100% absorbing material with unit cross-section. The particle source is at centre of sphere

P3 Fraction of particles escaping from rectangular box measuring 2×2×1 units containing a 100% absorbing material with unit cross-section. The particle source is at the centre of the box

P4 Mean track length in infinite volume for a scattering material with unit cross-section. The ratio of the scattering to total cross-sections is 0.5 (P4a), 0.75 (P4b) and 0.9 (P4c)

P5 Back scattering from a rectangular slab. The source and a point-flux detector (next-event estimator) are situated on the same side of the slab. The detector measures particles scattered by the slab from one group to the other.

P6 Transmission through a thick slab of infinite lateral extent. The slab is 5 MFPs thick and is divided longitudinally into 5 slices having importances of 1, 3, 9, 27 and 81, increasing with increasing distance from the source. Transmitted particles are measured using an analogue flux (track-length, P6a) and a point-flux (next-event, P6b) estimator.

5.2 Error Analysis

The 50 runs performed for each test problem allows an independent estimate of the QR error to be made. These errors, calculated at the 9 reporting points, can be compared with the error estimates made using the method described in section 3. Figure 3 plots the cumulative probability distribution for the ratio, r, of the latter error estimate to the former. The data are aggregated over the 6 test problems and over the 9 reporting points for each run; no significant differences were observed in the r distribution between problems or between reporting points.

Figure 3 shows that there is some bias in r, which has a median value of 0.89 and a mean value of 0.94. In other words, Snyder's method appears to slightly underestimate the true error. However, the bias is small compared to the variance in the error estimate. The standard deviation in $\log_{10}(r)$ is 0.19. In other words, for 68% of runs, the estimated error is within a factor of 1.55 of the correct value.

For problems P1, P2, P4a, P4b and P4c, the expectation values for the tally results can be calculated analytically. Comparison of the QR and analytical values showed that the QR results are unbiased within the limits of their calculated errors.

5.3 Test problem results

Figure 4 plots the pseudorandom and QR errors for each of the 6 test problems and their variants. A power-law curve of form $a \cdot N^b$ where N is the number of events is fitted to each set of errors. For the QR case, the exponent is determined from the data. For the pseudorandom case, the exponent is fixed at -0.5. The power-law relation gives a good description of the dependence of both the pseudo- and quasirandom simulation errors on N.

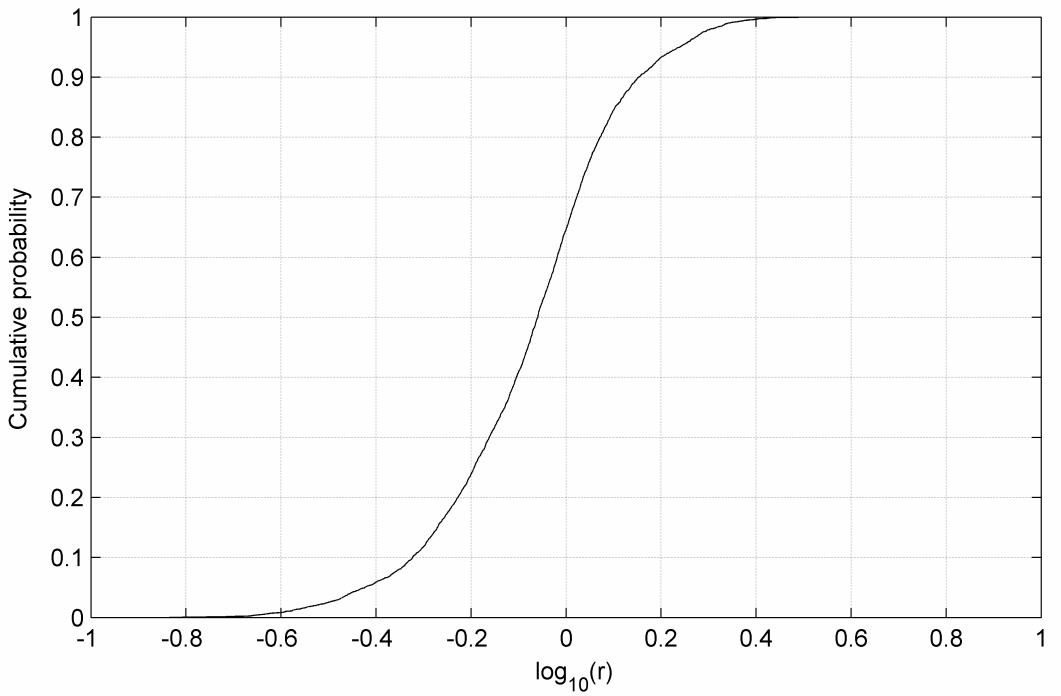

Figure 3. Cumulative probability plot for the ratio, *r*, of the estimated errors. See text for details of the definition of *r*.

Table 1 lists the ratios of the QR intercepts a_{QR} to the pseudorandom intercepts a_{PR} and the QR exponents b_{QR} for each problem. The errors on the exponents are estimated to be approximately ±0.02. Also shown is the quasirandom speed-up factor, *SF*, defined as the reduction in the number of events required using QR simulation to obtain the same error found using 10^6 pseudorandomly simulated events.

Table 1. Power-law coefficients and speed-up factor over pseudorandom simulation for the test problem suite.

	a_{QR}/a_{PR}	b_{QR}	*SF*
Problem 1	2.12	-0.93	270
Problem 2	1.10	-0.95	630
Problem 3	0.79	-0.70	72
Problem 4a	2.44	-0.90	180
Problem 4b	0.35	-0.69	200
Problem 4c	0.42	-0.52	10
Problem 5	0.89	-0.50	1.4
Problem 6a	0.64	-0.50	2.6
Problem 6b	0.80	-0.52	2.4

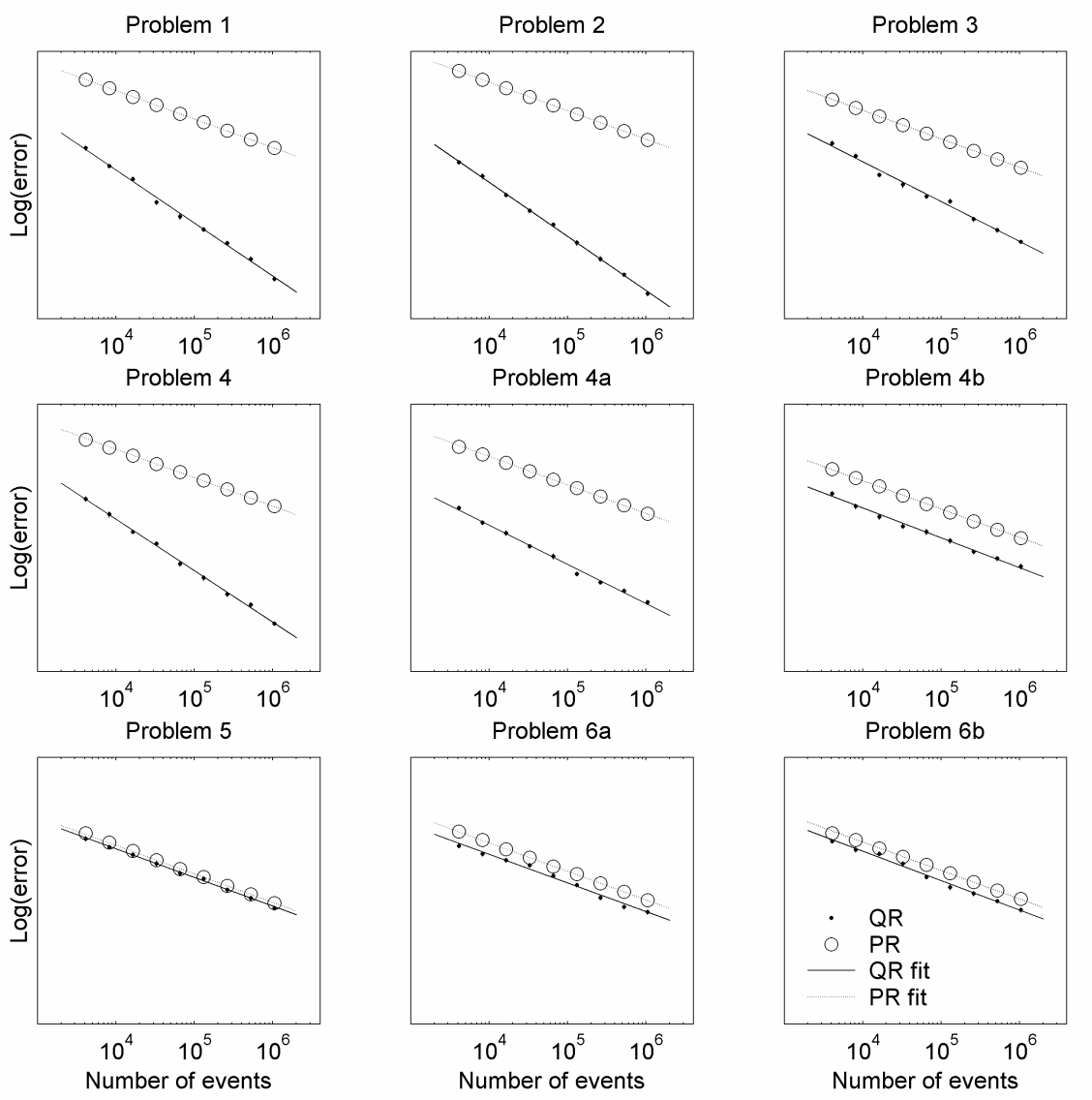

Figure 4. Comparison of quasirandom (QR) and pseudorandom (PR) errors for the 6 test suite problems and their variants. A power-law curve has been fitted to each data set.

5.4 Discussion

The greatest potential benefit from using QR rather than pseudorandom sequences for integration and simulation is the improved convergence rate. For both sequence types, the convergence with the number of events N (and hence time) is found to be well described by a power-law. The exponent, b, is -0.5 in the pseudorandom case and between -0.5 and -1.0 in the QR case.

The ideal result of b close to -1.0 is obtained for low-dimension, smooth integrands whose values are significant over a large fraction of the integral volume. Problem P1, which reduces to evaluating the integral $\int_0^\infty \exp(-x)\,dx$, is a good example of such a problem and has exponent b = -0.93. Increasing problem dimension and integrands that are discontinuous or

whose values are only significant over small regions of phase space generally reduce the rate of convergence [10,11].

Problem P2 is discontinuous but has finite variation as the discontinuity is restricted to a single dimension. The value of the exponent b = -0.95 remains close to -1.0.

Problem P3 has a 3-dimensional discontinuity as the probability of the particle escaping depends on the sampled values for the polar and azimuthal angles and the number of MFPs traveled. The variation is therefore infinite and Koksma-Hlawka inequality no longer applies. Berblinger *et al.*[11] argue that in such cases the integration error is dominated by points in the vicinity of the discontinuity. In an s-dimension problem with N sampled points, $N^{(s-1)/s}$ points are close to an *(s-1)*-dimension boundary. The carefully constructed, low-discrepancy nature of the QR sequences only applies for boundaries that are parallel to the coordinate axes; that is, for finite variation integrals. For other cases, it is essentially random on which side of the discontinuity a particular point will fall. Consequently, the $N^{(s-1)/s}$ boundary points contribute a relative integration error of $\sqrt{N^{(s-1)/s}}/N$, giving an exponent value of $b = -(s+1)/2s$. Problem P3 has an exponent of b = -0.70, which compares well with the predicted value of 0.667.

Problems 4a, 4b and 4c are all continuous and form a progression with increasing average dimension, with particles scattering on average 1, 3 and 9 times respectively. The exponent b decreases towards -0.5 with increasing problem dimension. However, even for the highest dimension problem 4c, the QR errors are substantially lower than the pseudorandom ones. Even though the exponent b = 0.52 implies an essentially pseudorandom rate of convergence, the ratio of intercepts is substantially less than unity. In other words, the use of QR sequences has effectively lowered the variance of the problem.

Similar results are observed for problems 5, 6a and 6b which all have multidimensional discontinuities. The fractions of particle trajectories that lead to a significant tally contribution are also small, particularly for the deep-penetration problem 6. For all three problems, the convergence exponent is consistent with the pseudorandom value of -0.5. However, somewhat lower errors are observed in the QR case due to the intercept ratio being less than one.

6 CONCLUSIONS

A 3-dimensional QR Monte Carlo neutral particle transport code using digit-scrambled Halton sequences has been demonstrated. For the simplest problems, the error is found to converge at a rate close to N^{-1} where N is the number of events generated. With runs of 10^6 pseudorandomly sampled events (relatively modest using today's computers), using QR sequences can reduce the time taken to achieve the same error by a factor of 100-600. For more realistic problems with discontinuities arising from boundaries between different materials, the convergence rate reduces to the pseudorandom result of $N^{-0.5}$. The use of QR sequences does leads to somewhat lower errors, effectively reducing the variance. However, the speed-up over pseudorandom simulation is fairly modest, typically only a factor of 1.5-3.

Further study of *variation* reduction methods for particle transport is required. For example, the analogue process of sampling the direction and distance-to-next-interaction after each collision invariably leads to infinite variation, as the polar coordinate frame used does not normally align with physical material boundaries. Modifications to the transport process, for

example by choosing the next interaction volume directly and then sampling the collision point inside this volume using an appropriate coordinate system could reduce a problem's variation.

QR techniques are most likely to be useful in the simplest problems and where high statistical accuracy is required. For problems with tallies dominated by direct source or low-order scattered contributions, a significant improvement in the convergence rate may be possible. Examples include collimator design studies, detector response function calculations and dose distribution modeling.

7 REFERENCES

1. F. James, J. Hoogland and R. Kleiss, "Multidimensional sampling for simulation and integration: measures, discrepancies and quasi-random numbers," *Comp. Phys. Comm.,* **99**, pp. 180-220 (1997)

2. J. H. Halton, "On the efficiency of certain quasi-random sequences of points in evaluating multi-dimensional integrals," *Numer. Math.*, **2**, pp. 84-90 (1960) and correction *ibid*, **2**, p. 196 (1960)

3. I. M. Sobol', "The distribution of points in a cube and the approximate evaluation of integrals," *USSR Comput. Math. Math. Phys.*, **7(4)**, pp. 86-112 (1967)

4. H. Faure, "Discrépance de suites associeés à un système de numeration (en dimension s)," *Acta Arith.*, **41**, pp. 337-351 (1982)

5. H. Niederreiter, "Low-discrepancy and low-dispersion sequences," *J. Number Theor.*, **30**, pp 51-70 (1988)

6. L. Kocis and W. J. Whiten, "Computation Investigations of Low-Discrepancy Sequences," *ACM Trans. On Math. Software, **23(2),*** pp. 266-294 (1997)

7. X. Wang and F. J. Hickernell, "Randomized Halton Sequences," *Math. and Comp. Model.*, **32**, pp. 887-899 (2000)

8. W. C. Snyder, "Accuracy estimation for quasi-Monte Carlo simulations," *Math. And Comp. in Simul.*, **54**, pp.131-143 (2000)

9. W. H. Press *et al*, *"Numerical Recipes in C"*, Cambridge University Press, Cambridge, UK (1992).

10. B. Moskowitz and R. E. Calflisch, "Smoothness and Dimension Reduction in Quasi-Monte Carlo Methods," *Mathl. Comput. Modelling*, **23(8/9)**, pp. 37-54 (1996)

11. M. Berblinger, Ch. Schlier and T. Weiss, "Monte Carlo integration with quasi-random numbers: experience with discontinuous integrands," *Comp. Phys. Comm.*, **99**, pp. 151-162 (1997)